PRECISION MEASUREMENTS OF HIGGS-BOSON PROPERTIES WITH THE ATLAS EXPERIMENT*

Martina Javurkova

on behalf of the ATLAS Collaboration

University of Massachusetts Amherst, Amherst, Massachusetts, USA

Received 24 March 2024, accepted 21 May 2024,
published online 5 August 2024

With the full Run 2 *pp* collision dataset collected at 13 TeV with the ATLAS detector, very precise measurements of Higgs-boson properties and its interactions can be performed, shedding light on the electroweak symmetry breaking mechanism. This contribution presents the latest measurements of the Higgs-boson properties by the ATLAS experiment in various decay channels, including differential, fiducial, and simplified template cross sections, mass, width, as well as their combination and interpretations. Specific scenarios of physics beyond the Standard Model are tested, as well as a generic extension in the framework of the Standard Model Effective Field Theory.

DOI:10.5506/APhysPolBSupp.17.5-A23

1. Introduction

The Standard Model (SM) of particle physics describes the known elementary particles and the forces that govern their interactions. An important feature of the SM is the spontaneous symmetry breaking in the electroweak sector which predicts the existence of a fundamental scalar boson, the Higgs boson, and allows particles to acquire mass by interacting with it. Its mass is not predicted by the theory, but once measured, the strengths of the interactions between the Higgs boson and other elementary particles can be precisely calculated. While theorised in the 1960s, the Higgs boson was first observed by the ATLAS and CMS collaborations at the Large Hadron Collider (LHC) at CERN in 2012. Precise measurements of its properties have since become one of the main goals of the research programme of the ATLAS experiment. Results from an unprecedented number of proton–proton collisions collected by the ATLAS detector at a centre-of-mass energy of $\sqrt{s} = 13$ TeV (Run 2 data-taking period between 2015 and

* Presented at the 30$^{\text{th}}$ Cracow Epiphany Conference on *Precision Physics at High Energy Colliders*, Cracow, Poland, 8–12 January, 2024.

2018), eventually combined with those from the Run 1 data-taking period from 2011 to 2012 performed at centre-of-mass energies of 7 and 8 TeV, are presented. In addition, some of the first measurements performed at the new world-record center-of-mass energy of $\sqrt{s} = 13.6$ TeV (Run 3 data-taking during 2022) are also reported.

2. Higgs-boson production and decay

At the LHC, Higgs bosons are primarily produced through gluon–gluon fusion process (ggF), which accounts for about 87% of Higgs-boson production, vector-boson fusion (VBF, where $V = W, Z$, 7%), associated production with vector bosons (VH, 4%), production in association with a pair of top quarks ($t\bar{t}H$, 1%), b-quarks ($b\bar{b}H$, 1%) or a single top quark (tH, 0.05%). Given that the measured value of the Higgs-boson mass is $m_H = 125$ GeV, the Higgs boson is predicted to decay dominantly into $b\bar{b}$ pairs with a branching ratio (BR) of 58%. There are seven following decay modes: decays into gauge boson pairs, *i.e.* W-boson pairs (22%), Z bosons (3%), photons (0.2%), Z boson and photon (0.2%), decays into fermion pairs, *i.e.* c-quarks (3%), τ-leptons (6%), and muons (0.02%).

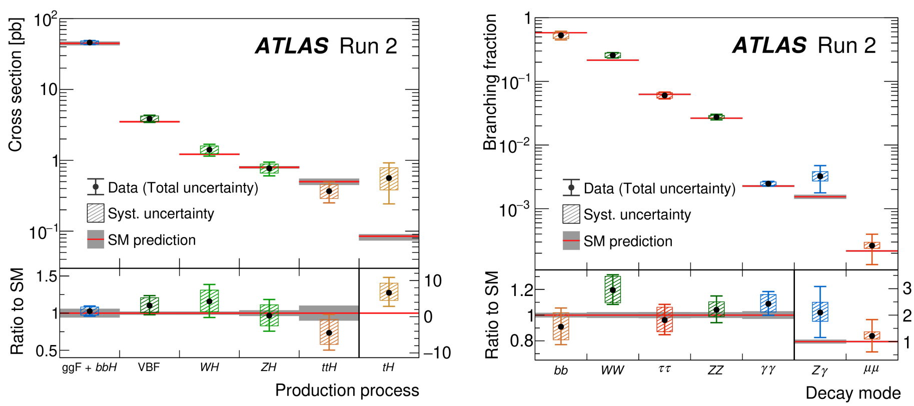

Fig. 1. Observed and expected Higgs-boson production cross sections (left) and branching fractions (right) [1].

The full Run 2 dataset, corresponding to an integrated luminosity of 139 fb^{-1} or pp collisions, is used for the measurements of Higgs-boson production and decay rates [1]. The production cross sections for ggF and VBF processes are measured with an accuracy of 7% and 12%, respectively. The WH, ZH production processes, and the combined $t\bar{t}H + tH$ production processes are now also observed with significances of 5.8σ, 5.0σ, and 6.4σ, respectively. The BRs of the $\gamma\gamma$, ZZ, WW, and $\tau\tau$ decays are measured with a precision of 10–12%. Despite being the dominant decay channel, the $b\bar{b}$ decay is very challenging experimentally and is therefore observed only now with a significance of 7.0σ. All results are compatible with the SM predictions and are shown in figure 1.

3. Higgs-boson coupling strength measurements

The cross-section and branching fraction measurements can be interpreted in terms of the strength of the interactions (or couplings) between the Higgs boson and a given particle p. These couplings are fully defined by the particle's mass and type and can be determined within the κ-framework [2] using a set of multiplicative coupling strength modifiers κ. They affect the Higgs-boson production ($\kappa_p^2 = \sigma_p/\sigma_p^{\mathrm{SM}}$) and decay ($\kappa_p^2 = \Gamma_p/\Gamma_p^{\mathrm{SM}}$) rates but do not alter any kinematic distributions of a given process. All measured coupling strength modifiers are shown in figure 2, where also the presence of non-SM particles in the loop-induced processes is allowed. These contributions are parametrised by effective coupling strength modifiers κ_g, κ_γ, and $\kappa_{Z\gamma}$. All values are found to be consistent with 1, indicating the compatibility with the SM expectations. When allowing invisible or undetected non-SM Higgs-boson decays to contribute to the total Higgs-boson width, upper limits are set at 95% C.L. on the corresponding BRs: $B_{\mathrm{inv}} < 0.13$ and $B_{\mathrm{u}} < 0.12$.

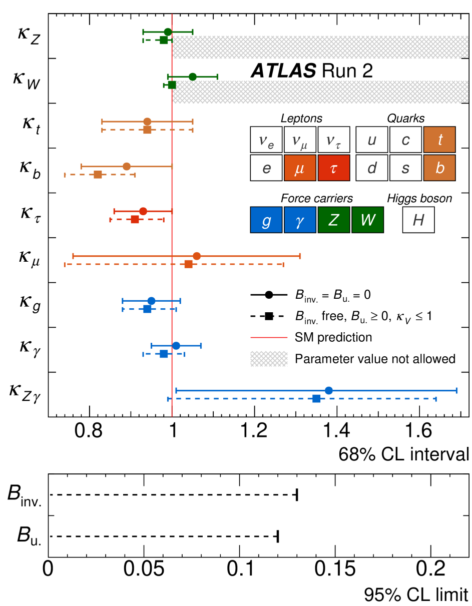

Fig. 2. Higgs-boson coupling strength modifiers and their uncertainties. The upper limits at 95% C.L. on B_{inv} and B_{u} are shown in the lower panel [1].

4. Higgs-boson cross-section measurements

Kinematic properties of the Higgs boson can be further scrutinised by performing measurements in different phase-space regions. Two complementary approaches are being pursued: measurements within the framework of simplified template cross sections (STXS) and fiducial cross-section measurements.

4.1. Simplified template cross section

The STXS framework [3] partitions the phase space into mutually exclusive regions. These kinematic cuts are defined for specific Higgs-boson production modes and inclusively in decay channels. This definition allows for a subsequent global combination of all measurements in different decay channels as well as from different experiments. All results of the simultaneous measurement of 36 kinematic regions using the full Run 2 data [1] are consistent with the SM predictions. The regions are probed also at high Higgs-boson transverse momenta, where the sensitivity to new physics is expected to be enhanced.

4.2. Fiducial cross section

Measurements of fiducial and differential cross sections in individual decay channels are performed in fiducial volumes defined at the particle level that closely matches the detector and analysis acceptance, which minimizes extrapolation effects. The measured cross sections are corrected for detector inefficiencies and resolution, through a procedure referred to as unfolding. Performing measurements at the particle level facilitates comparison with theoretical predictions. The differential fiducial cross sections are measured as a function of various variables sensitive to the properties of the Higgs boson. They are compared with fixed-order calculations at leading or higher order in quantum-chromodynamics (QCD) and electroweak (EW) perturbation order, as well as simulation matched to parton showers.

The first measurement of differential cross sections for the Higgs-boson production presented here is performed in the ggF channel and decay into $WW^* \to e\nu\mu\nu$ using the full Run 2 dataset [4]. The theoretical prediction as a function of the Higgs-boson transverse momentum is calculated at next-to-next-to-leading order (NNLO) in QCD. Final states with exactly two opposite-sign different-flavour leptons and at most one jet are considered. Additional requirements are imposed to suppress backgrounds, such as the removal of events containing a b-tagged jet with $p_{\mathrm{T}} > 20$ GeV, or to enhance the signal topology, for example, by selecting only events with the dilepton invariant mass smaller than 55 GeV. The differential cross sections are measured as a function of eight observables sensitive to the Higgs-boson production (the Higgs-boson transverse momentum: p_{T}^{H} and the rapidity of the leading jet: $|y_{j0}|$) and decay (the leading lepton's transverse momentum: $p_{\mathrm{T}}^{\ell 0}$, the dilepton system's transverse momentum: $p_{\mathrm{T}}^{\ell\ell}$, invariant mass: $m_{\ell\ell}$, rapidity: $y_{\ell\ell}$, azimuthal opening angle: $\Delta\phi_{\ell\ell}$, and $\cos\theta^{*}$ defined as $|\tanh(\frac{1}{2}\Delta\eta_{\ell\ell})|$). The number of signal events in each interval of the measured observables is extracted from a fit to the data in the distribution of the transverse mass. Figure 3 shows the cross sections as a function of p_{T}^{H} which is sensitive to fixed-order QCD (high-momentum region) as well as resummation effects and $|y_{j0}|$ which probes the theoretical modelling of quark and hard gluon emission. The results agree well with SM predictions, obtained using the POWHEG+PYTHIA 8, POWHEG+Herwig 7, and MadGraph5_aMC@NLO Monte Carlo (MC) generators. The dominant systematic uncertainties are related to jet and muon reconstruction, and background modelling.

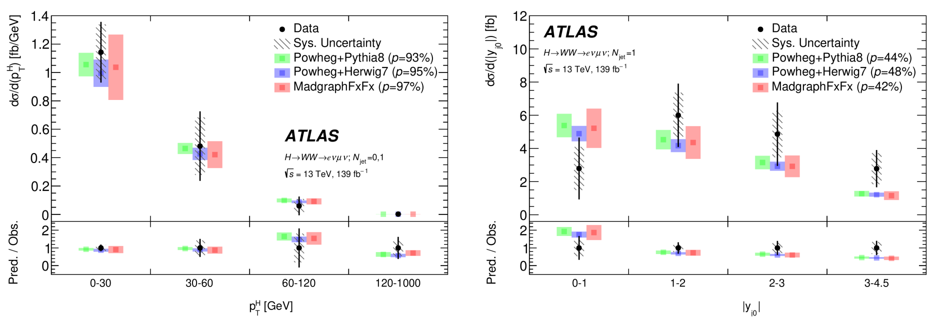

Fig. 3. Measured differential fiducial cross section for p_{T}^{H} (left) and $|y_{j0}|$ (right) compared to the SM predictions [4].

The fiducial integrated and differential cross sections are also measured in the VBF production of the $H \to WW^{*} \to e\nu\mu\nu$ channel using the full Run 2 dataset [5]. Events are required to contain exactly two different-flavour and opposite-sign charged leptons, and at least two high-p_{T} jets identified as originating from the VBF process. Additional selection requirements based on signal event kinematics and background event rejection are applied, such that the rapidity of the two tagged jets must be greater than 2.1. The signal yields are extracted from a fit to dedicated multivariate discriminant distributions in data. The integrated fiducial cross section is measured to be $\sigma_{\mathrm{fid}} = 1.68 \pm 0.33$ (stat.) $\pm\, 0.23$ (syst.) fb, which is consistent with the SM expectations that include NLO QCD and NLO EW corrections and with the LO QCD calculations with the parton showering, as shown in figure 4 (left). The differential cross sections are measured as a function of kinematic and angular observables of the final-state charged leptons and jets that are sensitive to the Higgs-boson production and decay properties. The measured cross sections are in good agreement with the POWHEG+PYTHIA 8 prediction, as shown in figure 4 (right) for the transverse momentum of the Higgs boson. The uncertainties in these measurements are dominated by the statistical uncertainty in data. Moreover, the measurements of differential cross sections are interpreted in the context of an Effective Field Theory (EFT) framework [6], where anomalous interactions of the Higgs boson to SM particles are introduced via additional dimension-six operators. The results are in good agreement with the SM predictions and constraints are set for various CP-even and CP-odd EFT parameters that are sensitive to the interactions between the Higgs boson and vector bosons, as well as CP-even parameters sensitive to the interactions with quarks.

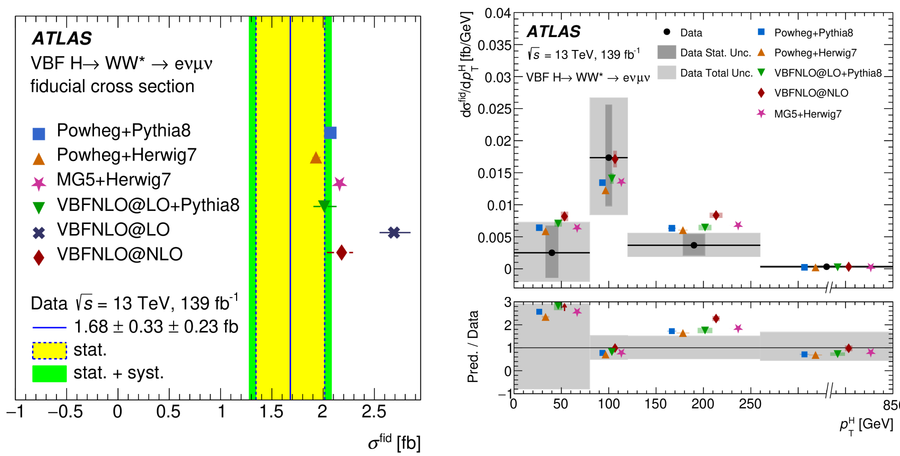

Fig. 4. Measured integrated (left) and differential fiducial cross section for $|y_{j0}|$ (right) compared to the theoretical predictions [5].

The only measurements reported here that use early Run 3 data at the new LHC center-of-mass energy of $\sqrt{s} = 13.6$ TeV collected in 2022 are the inclusive production cross sections measured in the $H \to \gamma\gamma$ (31.4 fb^{-1}) and $H \to ZZ^* \to 4\ell$ (29.0 fb^{-1}) decay channels [7]. Despite their low BRs, these two decay modes are interesting due to their excellent mass reconstruction, where the signal appears as a clear mass peak above a continuum background. The fiducial cross sections can therefore be extracted from a fit to the reconstructed $m_{\gamma\gamma}$ and $m_{4\ell}$ invariant mass spectra in data. Their values are measured to be $\sigma_{\mathrm{fid},\gamma\gamma} = 76^{+14}_{-13}$ fb and $\sigma_{\mathrm{fid},4\ell} = 2.80 \pm 0.74$ fb in the $H \to \gamma\gamma$ and $H \to ZZ^* \to 4\ell$ channels, which is in agreement with the corresponding SM predictions of 67.6 ± 3.7 fb and 3.67 ± 0.19 fb. Assuming SM values for the acceptances and the BRs of the two decay channels, these measurements are combined and extrapolated to the full phase space. The measured total Higgs-boson production cross section $\sigma(pp \to H) = 58.2 \pm 8.7$ pb agrees well with the SM expectation of 59.9 ± 2.6 pb, as shown in figure 5.

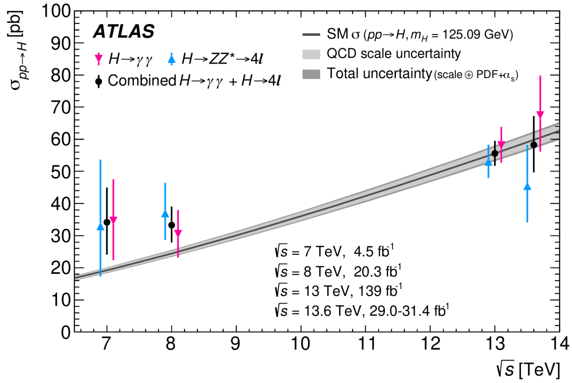

Fig. 5. Values of the Higgs-boson production cross section obtained from this and previous ATLAS measurements [8, 9] as a function of the pp centre-of-mass energy [7].

5. Measurements of the Higgs-boson mass

The Higgs-boson mass is the only free parameter of the scalar sector of the SM. Its precise measurement is of the highest importance as it provides a check of the internal consistency of the SM. Recently, the ATLAS Collaboration published an updated measurement of the Higgs-boson mass in the $H \to \gamma\gamma$ decay channel using the full Run 2 dataset [10]. Compared to the previous measurement based on the partial Run 2 dataset [11], the systematic uncertainty is reduced by a factor of four due to the improvements in the photon energy calibration. In addition, to increase the sensitivity, the selected events are classified into 14 mutually exclusive categories with different invariant mass resolutions and signal-to-background ratios. The Higgs-boson mass is measured to be 125.17 ± 0.11 (stat.) ± 0.09 (syst.) GeV.

This result is combined with the Run 2 ATLAS measurement in the $H \to ZZ^* \to 4\ell$ final state [12] and the measured value of the Higgs-boson mass is 125.10 ± 0.09 (stat.) ± 0.07 (syst.) GeV. A combination with the mass measurements using the Run 1 dataset is further performed and the combined result is $m_H = 125.11 \pm 0.09$ (stat.) ± 0.06 (syst.) GeV corresponding to a precision of 0.09%. A summary of these measurements is presented in figure 6.

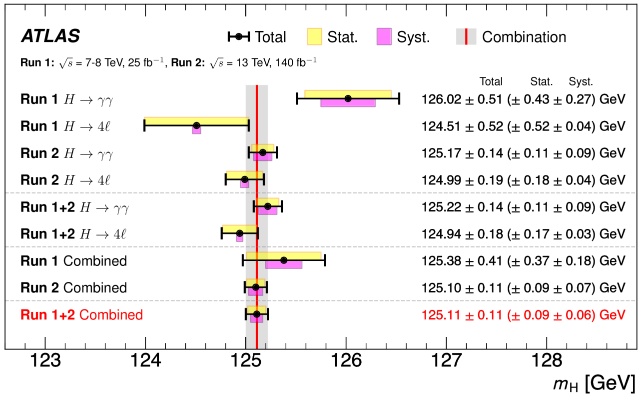

Fig. 6. Summary of m_H measurements from the $H \to \gamma\gamma$ and $H \to ZZ^* \to 4\ell$ decay channels and their combination [12].

6. Measurement of the Higgs-boson width

The total width of the Higgs boson is an important property of the SM, which is predicted to be 4.1 MeV. This value is too small to be measured directly from the line shape in the resonance region due to limited detector resolution. Therefore, a method has been developed to extract the total Higgs-boson width from the ratio of yields of observed events in the on-shell and off-shell Higgs-boson productions [13]. This measurement is performed in two final states, $ZZ \to 4\ell$ and $ZZ \to 2\ell 2\nu$, using the full Run 2 dataset [14]. In the 4ℓ channel, two multi-class dense Neural Networks (NNs) are trained to maximize the signal sensitivity in the ggF- and VBF-enriched regions, respectively. The observable from the first NN is shown in figure 7 (left). Assuming that the on-shell and off-shell coupling modifiers are the same for both production modes, the measured value of $\mathit{\Gamma}_H/\mathit{\Gamma}_H^{\mathrm{SM}}$ is found to be $1.1^{+0.7}_{-0.6}$, which corresponds to the total Higgs-boson width of $4.5^{+3.3}_{-2.5}$ MeV. The profile likelihood as a function of $\mathit{\Gamma}_H/\mathit{\Gamma}_H^{\mathrm{SM}}$ is shown in figure 7 (right). The data reject the background-only hypothesis with a significance of 3.3σ, representing evidence for the off-shell Higgs-boson production. No deviations from the SM expectations are observed. Since the off-shell Higgs-boson production is measured in the high-invariant mass region, it is expected to be sensitive to new physics beyond the SM. This measurement is therefore also used for the EFT interpretation [15]. Furthermore, the degeneracy of the Higgs–top quark and effective Higgs–gluon couplings is broken in the off-shell region, enabling the corresponding coupling modifiers to be measured separately. The associated Wilson coefficients are observed to be -1^{+19}_{-8} for $c_{t\varphi}$ (Higgs–top coupling modifier) and $0.00^{+0.03}_{-0.04}$ for $c_{\varphi G}$ (Higgs–gluon coupling modifier).

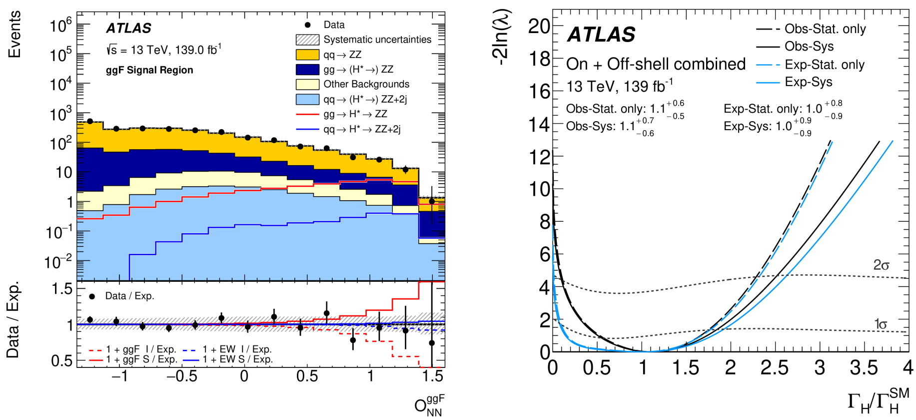

Fig. 7. The observed and expected SM distributions for the NN observable in the ggF signal region in the 4ℓ channel (left) and the likelihood profile as a function of $\Gamma_H/\Gamma_H^{\rm SM}$ for the combination with the on-shell measurement (right) [14].

7. Conclusion

After more than ten years since the discovery of the Higgs boson, we are entering the era of precision measurements of the Higgs-boson properties. The ATLAS Collaboration has observed all main production cross sections with a precision of 6% and the couplings to the weak bosons and the three heaviest fermions were measured with uncertainties ranging from 5% to 12%. The precision of the Higgs-boson mass reached 0.09% and the experimental evidence of off-shell Higgs-boson production was achieved. The integrated and differential cross-section measurements were performed in several channels and observables. The results are mostly dominated by statistical uncertainties and consistent with the most recent theoretical calculations. In addition to the results from the full Run 2 dataset, the measurements of the fiducial and total production cross sections using early Run 3 data collected in 2022 were also presented and found to be in agreement with the SM predictions.

REFERENCES

[1] ATLAS Collaboration, *Nature* **607**, 52 (2022).

[2] LHC Higgs Cross Section Working Group (S. Heinemeyer *et al.*), «Handbook of LHC Higgs Cross Sections: 3. Higgs Properties», CERN-2013-004.

[3] LHC Higgs Cross Section Working Group (D. de Florian *et al.*), «Handbook of LHC Higgs Cross Sections: 4. Deciphering the nature of the Higgs sector», CYRM-2017-002.

[4] ATLAS Collaboration (G. Aad *et al.*), *Eur. Phys. J. C* **83**, 774 (2023).

[5] ATLAS Collaboration (G. Aad *et al.*), *Phys. Rev. D* **108**, 072003 (2023).

[6] B. Grzadkowski, M. Iskrzyński, M. Misiak, J. Rosiek, *J. High Energy Phys.* **2010**, 85 (2010).

[7] ATLAS Collaboration (G. Aad *et al.*), *Eur. Phys. J. C* **84**, 78 (2024).

[8] ATLAS Collaboration (G. Aad *et al.*), *J. High Energy Phys.* **2023**, 028 (2023).

[9] ATLAS Collaboration (G. Aad *et al.*), *Phys. Rev. Lett.* **115**, 091801 (2015).

[10] ATLAS Collaboration, *Phys. Lett. B* **847**, 138315 (2023).

[11] ATLAS Collaboration, *Phys. Lett. B* **784**, 345 (2018).

[12] ATLAS Collaboration (G. Aad *et al.*), *Phys. Rev. Lett.* **131**, 251802 (2023).

[13] F. Caola, K. Melnikov, *Phys. Rev. D* **88**, 054024 (2013).

[14] ATLAS Collaboration, *Phys. Lett. B* **846**, 138223 (2023).

[15] ATLAS Collaboration, «Effective field theory interpretation of the measurement of off-shell Higgs boson production from $ZZ \to 4\ell$ and $ZZ \to 2\ell 2\nu$ decay channels with the ATLAS detector», ATL-PHYS-PUB-2023-012.